A PRACTICAL ENGINEERING APPROACH TO PREDICTING FATIGUE CRACK GROWTH IN RIVETED LAP JOINTS

Charles E. Harris*
Robert S. Piascik**
James C. Newman, Jr.***

An extensive experimental database has been assembled from very detailed teardown examinations of fatigue cracks found in rivet holes of fuselage structural components. Based on this experimental database, a comprehensive analysis methodology was developed to predict the onset of widespread fatigue damage in lap joints of fuselage structure. Several computer codes were developed with specialized capabilities to conduct the various analyses that make up the comprehensive methodology. Over the past several years, the authors have interrogated various aspects of the analysis methods to determine the degree of computational rigor required to produce numerical predictions with acceptable engineering accuracy. This study led to the formulation of a practical engineering approach to predicting fatigue crack growth in riveted lap joints. This paper describes the practical engineering approach and compares predictions with the results from several experimental studies.

INTRODUCTION

The ability to predict the onset of widespread fatigue damage in fuselage structures requires methodologies that predict fatigue crack initiation, crack growth, and residual strength. Mechanics-based analysis methodologies are highly desirable because differences in aircraft service histories can be addressed explicitly and rigorously by analyzing different types of aircraft and specific aircraft within a given type. The development of these advanced structural analysis methodologies has been guided by the physical evidence of the fatigue process assembled from coupons, laboratory lap joints panels, and from detailed tear-down examinations of actual aircraft structure.

Valid analytical methodology to predict the onset of widespread fatigue damage in fuselage structure must be based on actual observations of the physical behavior of crack initiation, crack growth, and fracture. The methodology presented herein is based largely on the results of teardown fractographic examinations of aircraft fuselage components. A large section of a fuselage containing a longitudinal lap joint extending for five bays was provided to NASA by an aircraft manufacturer after conducting a full-scale fatigue test [1]. A schematic of the panel is shown in Figure 1(a). The fatigue test was terminated after reaching the number of fuselage pressurization cycles that equaled approximately three times the original economic design life

* Center of Excellence in Structures and Materials, NASA Langley Research Center, Hampton, VA, USA
** Metals and Thermal Structures Branch, NASA Langley Research Center, Hampton, VA, USA
*** Mechanics and Durability Branch, NASA Langley Research Center, Hampton, VA, USA

goal of the aircraft established by the manufacturer. This section of the fuselage was selected because visual inspections, see Figures 1(b) and (c), made during the test had detected the growth of fatigue cracks extending from adjacent rivets which eventually linked up to form a long crack that extended completely across the bay. Further visual examinations of this section of the fuselage after completing the full-scale fatigue test suggested that this section contained multiple-site damage (a precursor to widespread fatigue damage). All rivet holes in each of the five bays of the panel were microscopically examined for fatigue cracks. The results of this examination form the physical basis for the analytical methodology developed by NASA to predict the onset of widespread fatigue damage.

The principal objective of the fractographic examination of the fuselage panel was to characterize multiple-site damage in a fuselage joint by assembling a database on the initiation and growth of fatigue cracks from rivets. Several general conclusions are obvious from the database [2]. First, fatigue cracks were present at virtually every rivet hole in the top row of rivets. The cracks ranged in size from about 50 micrometer to several centimeters. Crack initiation mechanisms included high local stresses, fretting along mating surfaces, and manufacturing defects created during the riveting process. The cracking behavior in each bay was similar and the results of the fatigue marker bands were relatively independent of rivet hole location. An example of small cracks found in the panel is shown in Figure 2. A small crack initiating due to high local stresses within the rivet hole is shown in Figure 2 (a). An example of a small crack initiating due to fretting is shown in Figure 2 (b). Figure 2 (c) shows a long crack that has been formed by the link up of the small fatigue cracks that developed at adjacent rivet holes. As can be seen in the photograph, the crack extended into the tear strap region, changed crack growth directions, and grew into a rivet hole in the tear strap. The surfaces of the individual fatigue cracks between the rivets were clearly identifiable in the fractographic examination of the long crack surface. Close examination revealed several cracks that initiated due to high local stresses and other cracks that initiated due to fretting. However, the lengths of all of the fatigue cracks at link up were approximately the same. This observation suggests that the long crack behavior is somewhat independent of the initiating mechanism. Furthermore, the quantitative data strongly suggest that the fatigue behavior of the long cracks is deterministic and predictable.

Based on the experimental evidence described above, the authors led the development of a comprehensive analysis methodology to predict the onset of widespread fatigue damage in lap joints of fuselage structure. Several computer codes were developed with specialized capabilities to conduct the various analyses the make up the comprehensive methodology. A full description of this methodology and the associated computer codes is given in reference 3. Over the past several years, the authors have interrogated various aspects of the analysis methodology to determine the degree of computational rigor required to produce analytical predictions with acceptable engineering accuracy. This study led to the formulation of a practical engineering approach to predicting fatigue crack growth in riveted lap joints. This practical engineering approach is the subject of this paper.

ENGINEERING APPROACH: ANALYSIS METHODOLOGY

In order to predict the fatigue life of a lap joint in a fuselage structure, the following global and local stress and fracture-mechanics analyses are required:

(1) global and local stress analyses of the lap joint in the fuselage structure,
(2) local elastic stress analyses of a rivet-loaded hole,
(3) stress-intensity factor analysis for cracks at critically-loaded rivet hole,
(4) fatigue analyses based on fracture mechanics and small crack theory, and
(5) residual strength analysis based on nonlinear fracture mechanics analyses.

It should be noted that these global and local analyses have been defined such that the load transfer through the riveted joint can be approximated by combining the results of the first four analyses. The authors recognize that the actual load transfer in the riveted joint is a very complex, nonlinear analysis problem. The sources of the nonlinear stress analysis behavior include the interaction between the rivet bearing contact, clamp-up and friction effects, interference fit stresses, bending effects, and crack growth. Rather than solving the fully nonlinear, three-dimensional problem, the above analyses were conducted in an interactive analysis scheme. Each of the five analyses will be described in detail in the following sections.

(1) Global and local stress analyses of the lap joint in the fuselage structure

To determine the load transfer in the lap joint of a fuselage structure, a global finite-element stress analysis is conducted using either the commercial codes (such as ABAQUS, ANSYS or MSC-NASTRAN) or the STAGS shell code [4]. In the current paper, the STAGS code was used for this purpose. The finite-element mesh shown in Figure 3 is a global model of a lap-joint region in a fuselage structure with stringers, frames, and shear clips modeled. The local model, Figure 3, shows the detailed lap-joint region with the riveted connections modeled with rigid links [4]. Fastener elements comprised of linear springs were used to model the mechanical connection between the layers at the rivet locations, as shown in the detailed model of the rivet in Figure 3.

(2) Local elastic stress analyses of a rivet-loaded hole

From the local stress analyses of the lap joint, the load distributions and by-pass loading is determined. For typical lap joints with 2, 3 and 4 rivet rows, finite-element analyses produce rivet loading (top rivet row) in terms of the local stress as 0.5, 0.37 and 0.29, respectively. For example, for the 3-rivet row, 37% of the load is carried by the rivet loading and 63% of the load is the by-pass loading [5].

The effects of secondary bending is determined from either the local elastic finite-element stress analysis of the lap joint or estimated from the Hartman-Schijve [6,7] bending equations. Three-dimensional (3D) stress analyses of a typical lap joint are presented in reference [8]. These analyses show good correlation of the calculated bending stresses from the 3D analyses with the Hartman-Schijve equations for elastic conditions. But if the applied stresses are high enough,

then local plastic yielding around the rivet hole rotates the joint and causes a dramatic reduction in the bending stresses.

For laboratory specimens, it has been found that rivet interference fit stresses are needed to predict the fatigue life of lap joints [9]. However, examination of fatigue test results on a full-scale fuselage test article [1] indicate that the riveted holes in the lap joint are in a neat-fit condition and interference is not needed to predict the fatigue crack growth rates.

(3) Stress-intensity factor analysis for cracks at critically loaded rivet hole

Fatigue life and fatigue crack growth predictions of riveted lap joints presented here uses a fracture-mechanics approach growing a crack from the micro-scale to failure. To make these calculations, the stress-intensity factors for corner and through cracks emanating from straight-shank rivet-loaded hole, as shown in Figure 4, subjected to rivet loading (P), by-pass stress (S_b), remote bending (M) and rivet interference (Δ) are needed. Stress-intensity factors have been calculated from finite-element analyses and some of these equations are given in reference 9.

To study the influence of the countersunk (100^o) rivet-hole configuration on stress-intensity factors, some recent analyses using the boundary-element method are shown in Figure 5 with some previous results on a straight-shank hole. Here the normalized stress-intensity factor is plotted against crack-length-to-hole radius (c/r). The open symbols are results for a straight crack in a straight-shank hole subjected to remote tension [10]. The solid circular symbol is for a straight crack in the countersunk configuration, as shown by the insert. The square symbols are for a circular crack with the center at the knife-edge of the countersink. Surprisingly, the results for a small crack in the knife-edge region gives about the same normalized stress-intensity factors for the straight or countersunk hole, presumably because of load transfer differences. The countersunk hole, near the knife-edge is thin and less stiff than the full thickness; thus more load would be shifted away from the knife-edge region. If the same load had gotten to the knife-edge region, then the stress-intensity factor should have been much greater than the straight-shank results. These results demonstrate that the corner crack at a straight-shank hole may also serve as an approximation for a crack at the countersunk hole.

(4) Fatigue analyses based on fracture mechanics and small crack theory

Because crack initiation effects are highly complex, fracture mechanics based life predictions have used the concept of an equivalent initial flaw size (EIFS) to capture the initiation process and start the problem at a reasonable flaw size [11]. To achieve accurate predictions, the EIFS must be chosen carefully. The EIFS should be based on a good understanding of the crack initiation processes associated with the specific crack problem being analyzed. Because the EIFS concept starts the problem at an assumed pre-existing level of damage, it does not mechanistically address the initiation process and when or at what rate the initiation damage occurs. For example, an EIFS used for fretting damage does not address when a critical level of fretting will cause crack initiation nor does it address local phenomenon, such as, the influence of fretting induced residual stress on small crack growth rates.

Small crack initiation and growth is a three-dimensional process with cracks growing in the depth and length directions interacting with the grain boundaries at different times in their cyclic history. Whereas a crack growing in the length direction may have decelerated at or near a grain boundary, the crack depth may still be growing. As the crack grows in the depth direction, the rise in the crack-driving force contributes to the crack penetrating that barrier. As the cracks become longer, the influence of the grain boundaries become less as the crack front begins to average behavior over more grains [12]. A probabilistic analysis would be required to assess the influence of the variability of the grain structure on crack growth rate properties. From an engineering standpoint, however, a weak-link of worst case scenario of grain orientation may provide a conservative estimate for the growth of small cracks through a complex microstructure. This is the basis for the continuum mechanics approaches.

It has been argued that the calculation of crack-tip stress intensity range factor (ΔK) for a small crack growing from a small defect could be in error [13]. For example, if crack initiation occurs at a subsurface inclusion with subsequent breakthrough to the surface, a considerable elevation in ΔK is possible over that calculated from the surface observations. Although the use of ΔK to characterize the growth of small cracks has proved to be convenient, its universal application has been viewed with some skepticism. Despite the above qualifications, research work on the growth of naturally initiated small cracks, notably by Lankford [12,14] and the AGARD studies [15,16], have demonstrated the usefulness of the ΔK concept.

One of the leading continuum mechanics approaches to small crack growth is that based on the crack-closure concept [17,18]. The crack-closure transient has long been suspected as a leading reason for the small crack effect. Crack closure modeling [19] has demonstrated the capability to model small crack growth behavior in a wide variety of materials and loading conditions [15-18]. Difficulties still exist for large-scale plastic deformations at holes or notches but these problems can be treated with advanced continuum mechanics concepts.

(5) Residual strength analysis based on nonlinear fracture mechanics analysis

The residual strength analysis of cracked 2024-T3 coupons, laboratory lap joints, structural test articles, and aircraft fuselages require non-linear and elastic-plastic fracture mechanics analyses. For the coupons and the laboratory lap-joint panels, a two-parameter fracture criterion (TPFC) [20] is used in the FASTRAN code to terminate the crack-growth analysis. For small width coupons and lap joints, the TPFC fracture criterion is very close to a net-section-equal-yield-stress failure criterion. For lap joints with multiple-site damage (MSD) cracking in large structural test articles to simulate fuselage panels [21], the STAGS (shell code) and the critical crack-tip-opening angle (CTOA) fracture criterion has been successfully used to predict stable tearing and residual strength. Herein, only the TPFC will be used to predict the failure of coupons and laboratory lap joints. It should be noted that the full-scale fuselage fatigue test articles was stopped at 66,000 pressure cycles and a residual strength analysis was not needed.

ENGINEERING APPROACH: PREDICTIONS

The “engineering approach” used for the lap joint fatigue life predictions made herein account for rivet load, by-pass load, secondary bending, simple rivet hole configuration, small-crack

behavior, and some environmental effects. The EIFS used for these predictions considers, but does not rigorously account for, the following effects on crack initiation and growth: rivet fit-up and interference fit stresses, residual stresses from multiple sources, manufacturing defects in the rivet joint, specific 3-D rivet-hole configuration, local stress concentrations at the micro-scale, fretting kinetics, cladding, and environmental (pitting corrosion and fretting-oxide debris) effects.

Laboratory Coupon Fatigue Test

Figure 6 shows a comparison of small-crack data [22] and large-crack data [23] for the 2024-T3 alloy. The small crack data, shown by the symbols, is only a small part of the overall database on this alloy. These results at R = 0 were taken in laboratory air conditions and at an applied stress level of 110 MPa. This alloy showed a very large difference between the large-crack threshold (about 3 MPa$\sqrt{m}$) and small-crack growth behavior. Small cracks grew at ΔK values as low as 0.7 MPa$\sqrt{m}$. But for ΔK values greater than 3 MPa$\sqrt{m}$, the small- and large-crack data agreed quite well. The solid curve is the predicted rates from the FASTRAN closure model using the baseline ΔK_{eff} – rate curve (dashed line). The initial defect was selected as a 6-μm radius surface crack located at the center of the notch. For the R = 0 condition, the initial drop in rates at a ΔK value of about 1 MPa$\sqrt{m}$ is quite small.

Piascik and Willard [24] conducted small-crack fatigue tests on notched specimens immersed in a salt-water solution on 2024-T3 aluminum alloy. These results are shown in Figure 7. (Note that the small-crack experiments were conducted in 1% NaCl solution and polarized to near the open circuit potential, -700 mV_{SCE}. This was done to preserve fracture surfaces and no appreciable difference in da/dN is likely compared to 3.5% NaCl solution). In Figure 7, the effective stress-intensity factor is plotted against rate. For tests conducted at stress ratios greater than or equal to 0.7, the ΔK values reported were assumed to be equal to ΔK_{eff}. But for the results at R = 0.05, the crack-opening stress level was assumed to be the same as that for laboratory air (like those used to analyze the data shown in Fig. 6). The solid lines were drawn through the mean of the test data under the salt-water solution. The dashed lines show the ΔK_{eff} – rate for the bare and alclad 2024-T3 under laboratory air conditions. The largest environmental effect is at low levels of ΔK where a factor of 5 increase in salt-water rates compared to air rates (dashed line) is observed at a ΔK of 1 MPa$\sqrt{m}$. But at a ΔK of approximately 7 MPa$\sqrt{m}$, salt-water and laboratory-air rates converge; here, the fatigue crack growth rates are fast and crack-tip environmental effects are minimized.

Landers and Hardrath [25] determined the fatigue lives of 2024-T3 aluminum alloy specimens with a central hole under laboratory air conditions. The results for specimens with a hole radius of 1.6 mm and tested at two stress ratios are shown in Figure 8. The symbols with arrows indicate that the test was stopped before failure. The curves are the predicted results using an initial semi-circular crack size (6 μm) that had an equal area to the average inclusion-particle sizes that initiated cracks [1]. The analyses tended to under predict lives for R = 0 and slightly over predict lives for R = -1. The influence of stress ratio on fatigue limits was predicted quite well using a value of $(\Delta K_{eff})_{th}$ of 0.75 MPa$\sqrt{m}$ (determined from the un-notched specimens [26]). Note that for aluminum alloys the fatigue limit is not well defined and the ΔK_{eff} – rate

curve in Figure 6 might have a steep slope for rates below 1 x 10^{-8} mm/cycle instead of having a sharp cutoff.

Laboratory Panel Lap Joint Fatigue Test: Straight-shank rivets

A series of tests were conducted by Hartman [27] to study the fatigue behavior of simple riveted lap joints with straight-shank rivets under laboratory air and room temperature conditions for constant- and variable-amplitude loading. The test specimens were flat unstiffened panels with a joint formed by two overlapping sheets attached by two rows of rivets loaded in single shear, as shown in Figure 9. The sheets were aluminum alloy 2024-T3 Alclad at a nominal sheet thickness of 1 mm and the rivets were 2024 (type DD). The straight shank, button-head rivets had a diameter of 3.2 mm. In all tests, a constant mean stress was applied corresponding to a nominal gross tensile stress of 68.6 MPa. Constant-amplitude fatigue tests were conducted under alternating stresses ranging from a high of 67 MPa to a low of 16 MPa. At least two replicate fatigue tests were conducted for each loading condition. These alternating stresses resulted in fatigue lives from about 40,000 to over 30 million cycles to failure. In the variable-amplitude fatigue tests, specimens were subjected to a block-program loading sequence containing eleven different stress-amplitude blocks composed of a total of 59,300 cycles.

The general conclusion by Hartman [27] was that the riveting procedure, hydraulic, pneumatic, hand driven, or riveting machine, did not appear to have a significant effect on fatigue life. Several series of tests were purposely designed to achieve a larger rivet head diameter producing higher interference and clamp-up stresses. The first and second test series had a rivet-head diameter from 5.0 to 5.2 mm and 5.4 to 5.8 mm, respectively. At each stress amplitude, about twenty fatigue tests were conducted but the scatter was remarkably small considering such a complex joint and the many manufacturing variables studied. (These results will be shown later.) While the fatigue data from these two sets of test series did overlap, the large diameter rivet heads resulted in a mean fatigue life that was about a factor of 2 higher than the mean fatigue life for the specimens with the smaller diameter rivet heads.

Because the outer rivets carry a higher rivet load, these holes are expected to crack earlier than the other holes [9]. Thus, the failure progression starts with small corner cracks (6 μm) located at the edge of the rivet hole and faying surface for the outer rivets, the corner cracks propagates through the thickness, and then the through cracks propagate until the K value for the rivet-loaded crack is equal to that for a double-edge crack subjected to only remote stress. Failure will occur when the fracture toughness of the material is exceeded. The “effective” interference will then be selected to fit test data on the lap joints under constant-amplitude loading. Then the same initial crack size and interference level will be used to predict the fatigue behavior under the block-program loading.

A comparison between the measured and calculated fatigue lives for the NLR lap joints with a rivet-head diameter of 5.1 are shown in Figures 10. The dashed curves are the predicted fatigue lives based on “no interference” with an initial flaw size of 6 μm. The interference level was selected by trial-and-error to fit the experimental test data for each data set. The interference levels were 5.8 μm for the 5.1-mm rivet-head diameter. The calculated fatigue lives agreed well with the mean of the test data on the lap joints. However, if a larger flaw size had been selected,

then the interference level needed to fit these test data would have also been larger because the no-interference life calculations would have been shorter than the present calculated lives. Although these levels of interference are very low, in comparison to quoted values in the literature, the rivet can only exert an "elastic" spring-back on the rivet hole. Depending upon the level of radial pressure exerted by the rivet (yield stress to several times the yield stress), some estimates of the elastic spring-back ranged from 4 to 16 μm's.

Hartman [27] conducted a large number of fatigue tests on the same type of lap joint under block-program loading for the same manufacturing conditions as the constant-amplitude tests. The block-program loading had eleven different stress amplitudes (constant mean stress) for a low-high-low sequence for 59,300 cycles. The measured fatigue lives under the repeated block-program loading are shown in Figure 11 as open and solid symbols for the two rivet-head diameters, respectively. Although the test results showed a large amount of scatter, the larger rivet-head diameter produced a slightly longer fatigue life than the smaller rivet-head diameter tests, similar to the constant-amplitude results. The dotted line shows the predicted life with no interference ($\Delta = 0$). The solid and dashed lines are predicted lives using the two levels of interference determined from the constant-amplitude tests. These predicted results are very close to the mean life obtained from the test on each rivet-head diameter. These comparisons demonstrate the capability to analytically predict fatigue lives of riveted lap joints based solely on crack propagation and small-crack theory.

Laboratory Panel Lap Joint Fatigue Test: Countersunk rivets

A series of tests were conducted by Furuta, Terada and Sashikuma [28] to study the fatigue behavior of countersink riveted lap-joint panel exposed to laboratory air or to a corrosive salt water environment. Figure 12 shows the configuration of the four types of 2024-T3 (Aclad) panels tested: Type 1 - two rivet row, Type 2 - three rivet row, Type 3 – three rivet row with thin-straight tear straps, and Type 4 – three rivet row with non-uniform thick tear straps. Testing was conducted at constant amplitude loading which simulated the fuselage skin stress. Tests were conducted under ambient (laboratory air and room temperature) conditions and under a corrosive environment. For the corrosive environment, the lap-joint panels were immersed in circulating 3.5% NaCl solution.

The remote stress due to rivet load (S_p), by-pass stress (S_b) and remote bending stresses (S_M) were used in the life analyses of the Furuta [28] panels. An interference level was not used in any calculations ($\Delta = 0$). The two-rivet row (Type 1) had a 50% rivet and by-pass stress; whereas, the three-rivet row (Types 2-4) had 37% rivet stress and 63% by-pass stress. Only Type 1 was considered with and without bending. Schijve's [7] rivet-rotation correction bending equations were used to estimate the bending stresses. Based on 3-D stress analyses in reference 9, the applied stress level of 96 MPa, in the Furuta panel, should have yielded the rivet hole and greatly reduced the bending effects.

Figure 13 shows that the fatigue-life of Type 1 panels exposed to salt water (square symbol) is reduced by a factor of about 1/2 or 1/3 compared to the fatigue-life in ambient laboratory air (circle symbol). The FASTRAN predictions, for salt water (dashed line) and laboratory air (solid line) environments are in excellent agreement with the experimental results. Here, the fracture

mechanics based calculations assumed a corner crack in a neat-fit riveted-loaded straight shank hole (rivet fit-up and interference fit stresses are assumed small). The 6 μm radius EIFS used for each FASTRAN prediction is consistent with laboratory observations; 6 μm radius constituent particles and corrosion pits are observed at small crack initiation sites in fatigue test coupons exposed to laboratory air and salt water, respectively [18, 25]. Figure 14 shows that the "engineering approach" accurately predicts the fatigue life for all panel configurations and environments. The FASTRAN predicted (solid circle) fatigue lives shown in Figure 14 are in excellent agreement with Fututa et al test results (open circle).

Full-Scale Fuselage Test Article

The "engineering approach" was used to predict the total fatigue life of the full-scale fuselage test article previously described in the Introduction [1,2]. The experimentally determined crack growth rate data from 3 panels and 7 bays are plotted in Figure 15. The test results include data from both counter bore and straight shank rivet hole configurations. It is obvious that the data is well behaved and suggests that fatigue crack growth is deterministic and predictable. Figure 16 compares the test results obtained from the full-scale test article destructive examination and FASTRAN predictions. Two distinct populations are shown in Figure 16, the open circle data are those cracks that initiated first and grew to longer lengths and the solid symbols are smaller cracks that initiated later in life. The predictions are based on engineering estimates of remote stress (PR/t), bending stress (Schijve's approximation), and by-pass loading (29% for a four rivet row lap joint). In keeping with the "engineering approach", the neat pin / straight shank hole / corner crack configuration was used to calculate crack-tip stress intensity factors. An EIFS was selected based on the results of the detailed destructive examination; here, the majority of fatigue cracks initiated by a fretting damage located in the faying surface clad (reference) and therefore, an EIFS of 50 μm, the nominal thickness of the clad, was selected. The FASTRAN (50 μm) prediction is in excellent agreement with fatigue cracks that initiated later in life. Also shown in Figure 16 is a prediction based on an EIFS of 100 μm; here, the calculated results reasonably predicts the life of the lap joint that exhibited much greater fretting damage and cracks that initiated earlier in life. The third prediction shown in Figure 16 used an EIFS (6 μm) identical to that used for the Furuta et al panel prediction discussed above. The 6-μm EIFS results in a prediction that substantially over predicts the total fatigue life of the fuselage lap joint, suggesting that the effects of fretting on total fatigue life are substantial.

CONCLUDING REMARKS

An extensive experimental database has been assembled from very detailed teardown examinations of fatigue cracks found in the rivet holes of several fuselage structural components. The primary observation from an examination of this experimental database is that the fatigue crack growth behavior is well behaved and, therefore, predictable using a deterministic methodology. Based on the results of this experimental study, the authors led the development of a comprehensive analysis methodology to predict the onset of widespread fatigue damage in lap joints of fuselage structure. Several computer codes were developed with specialized capabilities to conduct the various analyses the make up the comprehensive methodology. The authors interrogated various aspects of the analysis methodology to determine the degree of computational rigor necessary to generate analytical predictions with acceptable engineering

accuracy. It was found that some very complicated aspects of the analysis methodology could be simplified without a significant loss in computational accuracy. The simplifications to the analysis are those typically used by practicing engineers. For example, it was found that the residual stresses due to rivet interference fit had a second order effect on the fatigue crack growth in the fuselage components included in this study. Therefore, the stress intensity factors used in the fatigue crack growth calculations could be accurately determined by compounding the linear, elastic solutions for the individual loading components. These observations led to the formulation of a practical engineering approach to predicting fatigue crack growth in riveted lap joints. Comparisons of the analytically predicted fatigue crack growth values were in close agreement to the experimental results. Furthermore, an equivalent initial flaw size engineering (EIFS) approach was found to be quite suitable for predicting total fatigue life of coupons, panels, and fuselage components. However, the EIFS must be determined for each unique combination of structural geometry and service environment.

REFERENCES

1. Piascik, R. S. and Willard, S. A., "The Growth of Multi-Site Fatigue Damage in Fuselage Lap Joints", Second Joint NASA/FAA/DoD Conference on Aging Aircraft, NASA/CP-1999-208982, National Aeronautics and Space Administration, Washington, D.C., 1999, pp. 397-407.

2. Piascik, R. S. and Willard, S. A., 'The Characterization of Fatigue Damage in the Fuselage Riveted Lap Splice Joint", NASA/TP-97-206257, National Aeronautics and Space Administration, Washington, D.C., 1997.

3. Harris, C. E.; Newman, J. C., Jr.; Piascik, R. and Starnes, J. H., Jr., "Analytical Methodology for Predicting the Onset of Widespread Fatigue Damage in Fuselage Structure", Journal of Aircraft, Vol. 35, No. 2, 1998, pp. 307-317.

4. Rankin, C. C.; Brogan, F. A.; Loden, W. A. and Cabiness, H. D., "STAGS User Manual - Version 2.4," Lockheed Martin Advanced Technology Center, Report LMSC P032594, 1997.

5. Muller, R. P. G., "An Experimental and Analytical Investigation on the Fatigue Behaviour of Fuselage Riveted Lap Joints," Ph.D. Thesis, Delft University of Technology, The Netherlands, 1995, p. 161.

6. Hartman, A. and Schijve, J., "The Effect of Secondary Bending on Fatigue Strength of 2024-T3 Alclad Riveted Joints", NLR TR 69116 U, 1969.

7. Schijve, J., "Some Elementary Calculations on Secondary Bending in Simple Lap Joints", NLR TR 72036 U, 1972.

8. Newman, J. C., Jr. and Raju, I. S., "Stress-Intensity Factor Equations for Cracks in Three-Dimensional Finite Bodies subjected to Tension and Bending Loads", Computational Methods in Mechanics of Fracture, S. N. Atluri, (ed.), Elsevier, 1986, pp.311-334.

9. Newman, J. C., Jr.; Harris, C. E.; James, M. A. and Shivakumar, K. N., “Fatigue-Life Prediction of Riveted Lap Joints using Small-Crack Theory,” Fatigue in New and Ageing Aircraft, R. Cook and P. Poole, (eds.), EMAS Publishing, 1997, pp. 523-552.

10. Newman, J. C., Jr.; Wu, X. R.; Venneri, S. L. and Li, C. G., “Small-Crack Effects in High-Strength Aluminum Alloys,” NASA RP-1309, May 1994.

11. Rudd, J. L., Yang, J. N., Manning, S. D. and Garver, W. R., "Durability Design Requirements and Analysis for Metallic Structures," Design of Fatigue and Fracture Resistant Structures, ASTM STP 761, P. R. Abelkis and C. M. Hudson, (eds.), 1982, pp. 133-151.

12. Lankford, J., “The Growth of Small Fatigue Cracks in 7075-T6 Aluminum”, Fatigue of Engineering Materials and Structures, Vol. 5, 1982, pp. 233-248.

13. Schijve, J., “The Practical and Theoretical Significance of Small Cracks – An Evaluation,” Fatigue 84, EMAS Ltd., 1984, pp. 751-771.

14. Lankford, J., “The Effects of Environment on the Growth of Small Fatigue Cracks”, Fatigue Engineering Materials and Structures, Vol. 6, 1983, pp. 15-32.

15. Edwards, P. R. and Newman, J. C., Jr., (eds.), “Short-Crack Growth Behavior in Various Aircraft Materials”, AGARD R-767, 1990.

16. Newman, J.C., Jr., “A Nonlinear Fracture Mechanics Approach to the Growth of Small Cracks”, Behavior of Short Cracks is Airframe Components, H. Zocher, (ed.), AGARD CP-328, 1983, pp. 6.1-6.26.

17. Newman, J.C., Jr.; Swain, M. H. and Phillips, E.P., “An Assessment of the Small-Crack Effect for 2024-T3 Aluminum Alloy”, Small Fatigue Cracks, The Metallurgical Society, Inc., Warrendale, PA, 1986, pp.427-452.

18. Newman, J.C., Jr., “A Crack Closure Model for Predicting Fatigue Crack Growth Under Aircraft Spectrum Loading”, Methods and Models for Predicting Fatigue Crack Growth Under Random Loading, ASTM STP 748, 1981, pp. 53-84.

19. Newman, J. C., Jr., “Fracture Analysis of Various Cracked Configurations in Sheet and Plate Materials,” Properties Related to Fracture Toughness, ASTM STP 605, American Society for Testing and Materials, 1976, pp. 104-123.

20. Seshadri, B. R. and Newman, J. C., Jr., “Residual Strength Analyses of Riveted Lap-Splice Joints,” Fatigue and Fracture Mechanics: Thirty-First Volume, ASTM STP 1389, G. R. Halford and J. P. Gallagher, Eds., American Society for Testing and Materials, West Conshohocken, PA, 1999.

21. Young, R. D.; Rouse, M.; Ambur, D. R. and Starnes, J. H., Jr., “Residual Strength Pressure Tests and Nonlinear Analyses of Stringer- and Frame-Stiffened Aluminum Fuselage Panels with Longitudinal Cracks,” Second Joint NASA/FAA/DoD Conference on Aging Aircraft, C. E. Harris, (ed.), Williamsburg, VA., 1998, pp. 408-426.

22. Newman, J.C., Jr. and Edwards, P. R., “ Short-Crack Growth Behavior in an Aluminum Alloy – An AGARD Cooperative Test Programme”, AGARD R-732, 1988.

23. Phillips, E. P., “The Influence of Crack Closure on Fatigue Crack Growth Thresholds in 2024-T3 Aluminum Alloy”, ASTM STP 982, 1988, pp. 505-515.

24. Piascik, R. S. and Willard, S. A., “The Growth of Small Corrosion Fatigue Cracks in Alloy 2024,” Fatigue and Fracture of Engineering Materials and Structures, Vol. 17, No. 11, 1994, pp. 1247-1259.

25. Landers, C. B. and Hardrath, H. F., “Results of Axial-Load Fatigue Tests on Electropolished 2024-T3 and 7075-T6 Aluminum Alloy Sheet Specimens with Central Hole,” NACA TN-3631, 1956.

26. Newman, J. C., Jr., Phillips, E. P. and Swain, M. H., “Fatigue-Life Prediction Methodology using Small-Crack Theory,” International Journal of Fatigue, Vol. 21, 1999, pp. 109-119.

27. Hartman, A., “The Influence of Manufacturing Procedures on the Fatigue of 2024-T3 Alclad Riveted Single Lap Joints”, NLR TR 68072 U, July 1968.

28. Furuta, S.; Terada, H. and Sashikuma, H., “ Fatigue Strength of Fuselage Join Structures Under Ambient and Corrosive Environment”, ICAF 97 – Fatigue in New and Ageing Aircraft, EMAS Ltd., West Midlands, UK, 1997, pp. 231-249.

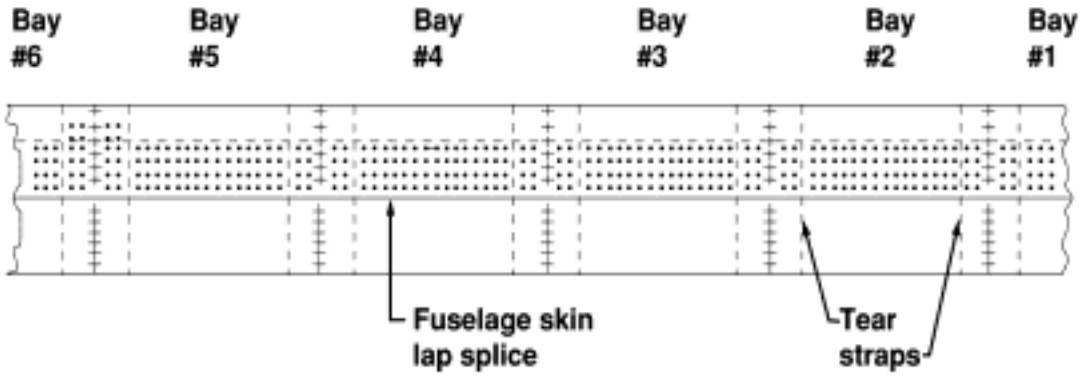

(a) Schematic of fuselage lap-joint panel

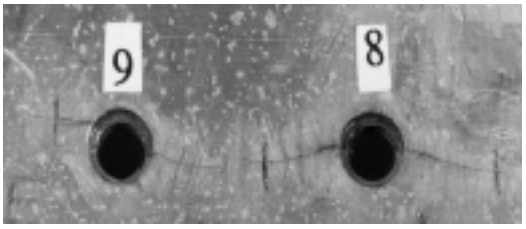

(b) Cracks extending from rivets

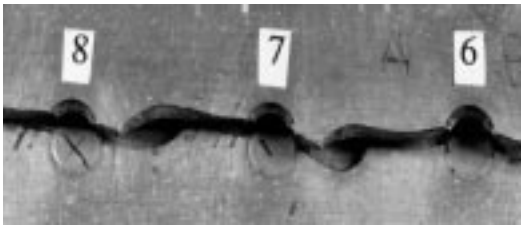

(c) Large crack in panel

Figure 1. – Teardown examinations of actual aircraft panels with riveted lap joints.

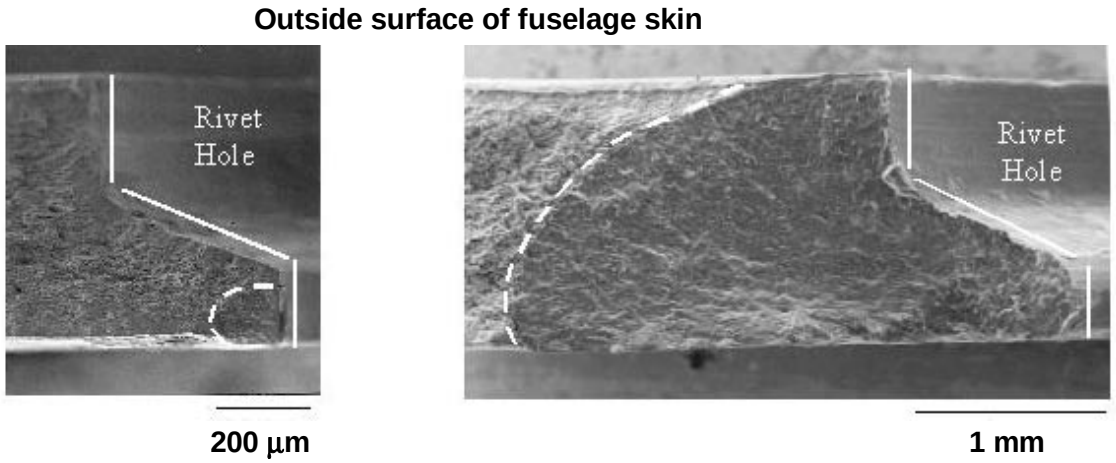

(a) Crack initiation due to high local stress.

(b) Crack initiation due to fretting (dashed line indicates crack front).

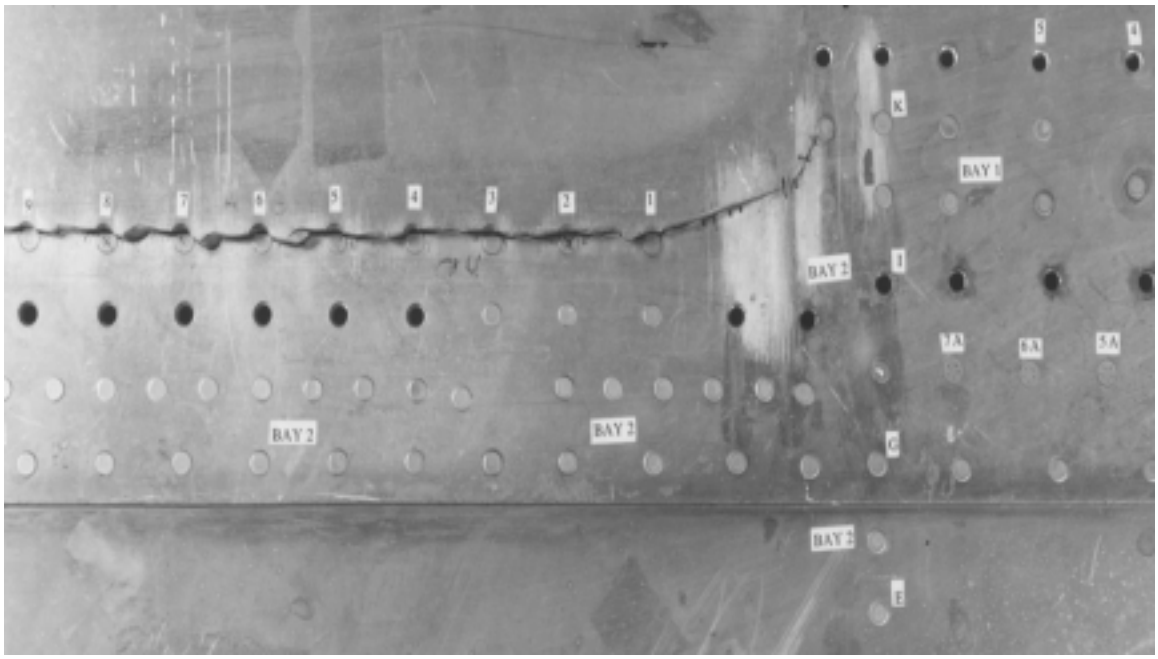

(c) Large crack formed by the link-up of fatigue cracks at adjacent rivets.

Figure 2. – Progression of damage in full-scale fatigue test article from small crack at rivet hole to link-up of multiple-site damage cracks and a large crack.

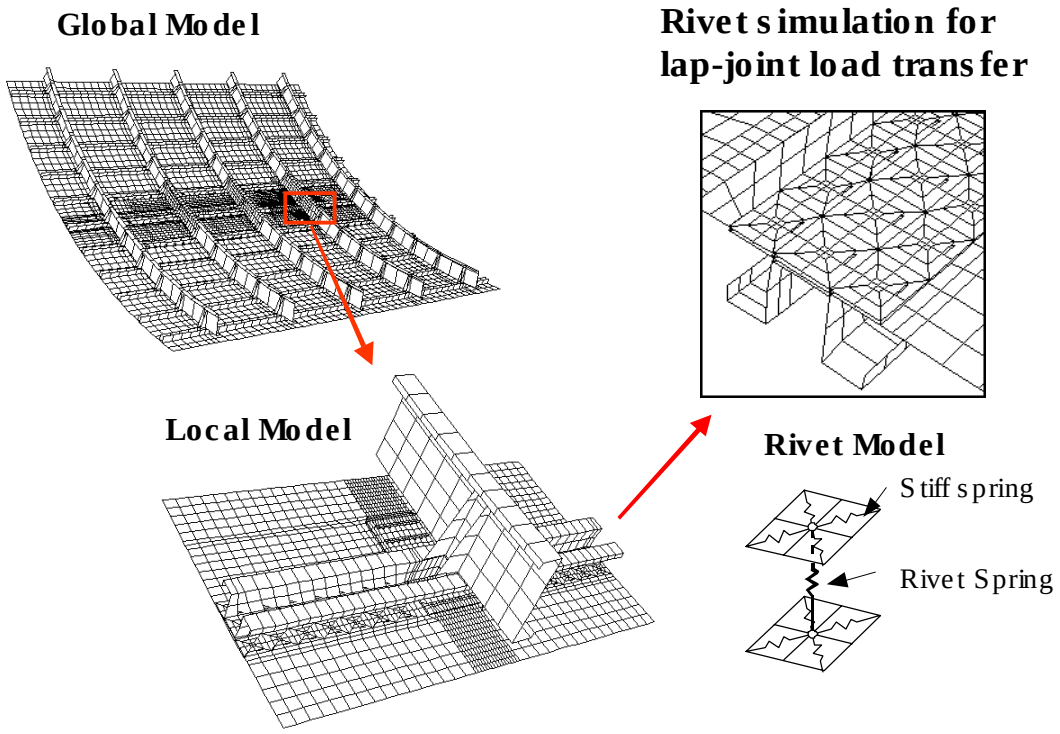

Figure 3. – Global and local finite-element models of lap joint in fuselage structure.

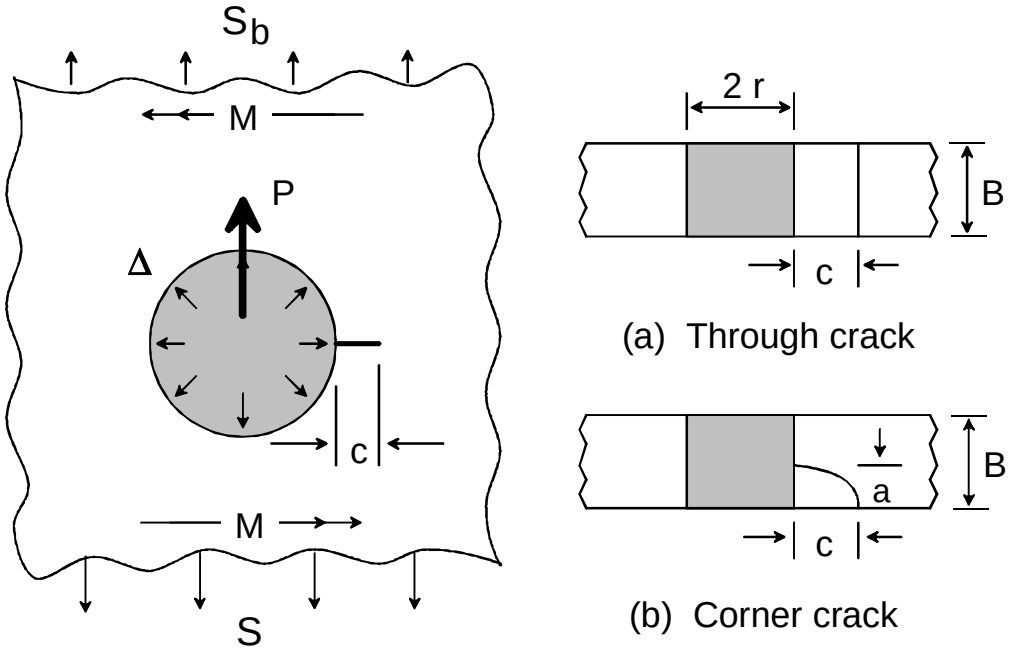

Figure 4. – Corner and through crack at riveted fastener hole under various loadings.

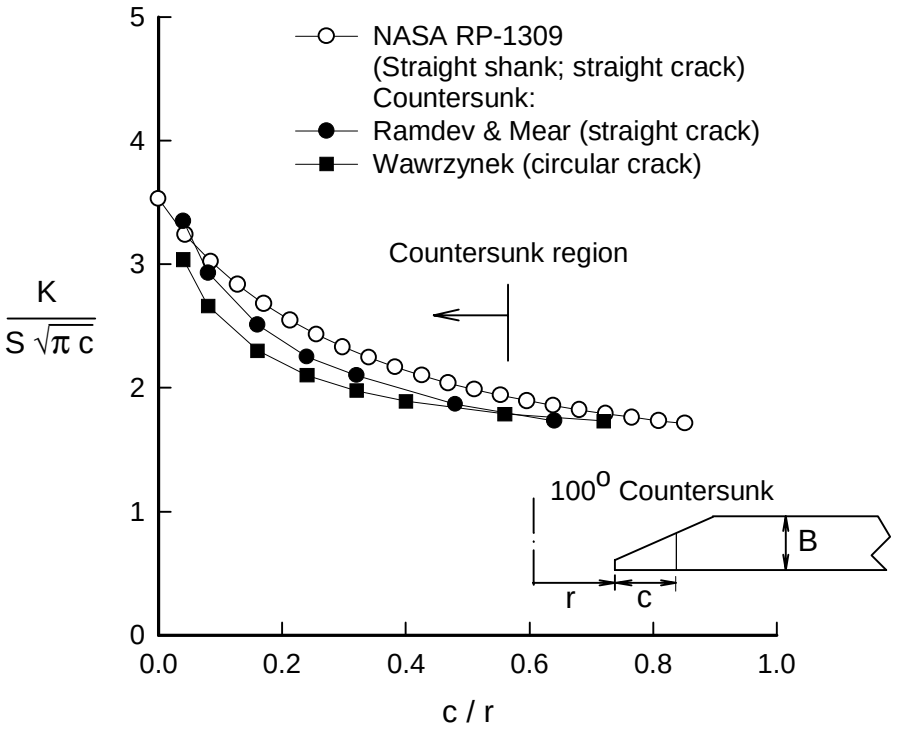

Figure 5. – Normalized stress-intensity factors for cracks at countersunk notch.

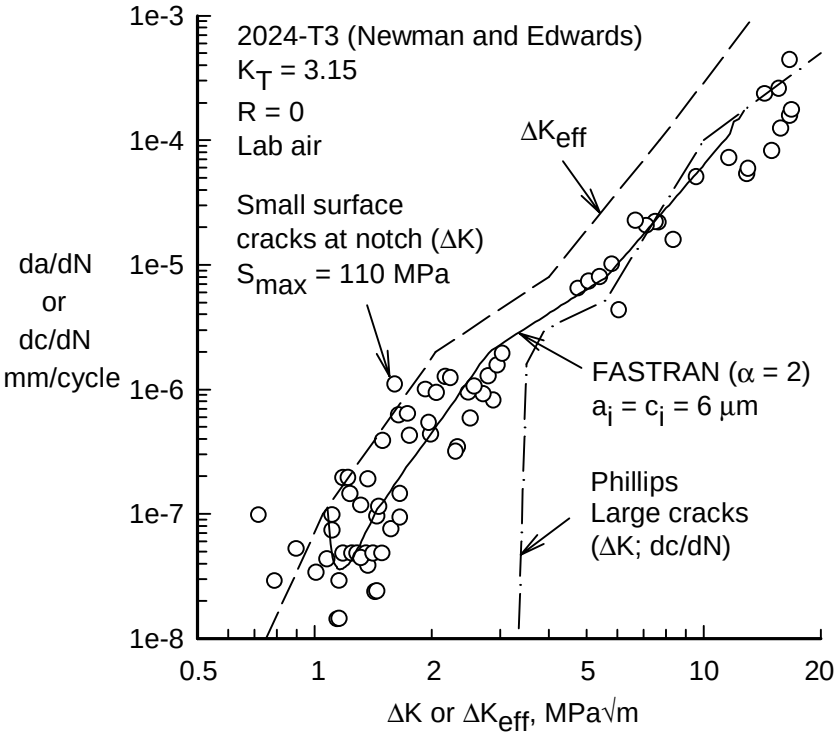

Figure 6. – Small-crack growth rate behavior in 2024-T3 aluminum alloy.

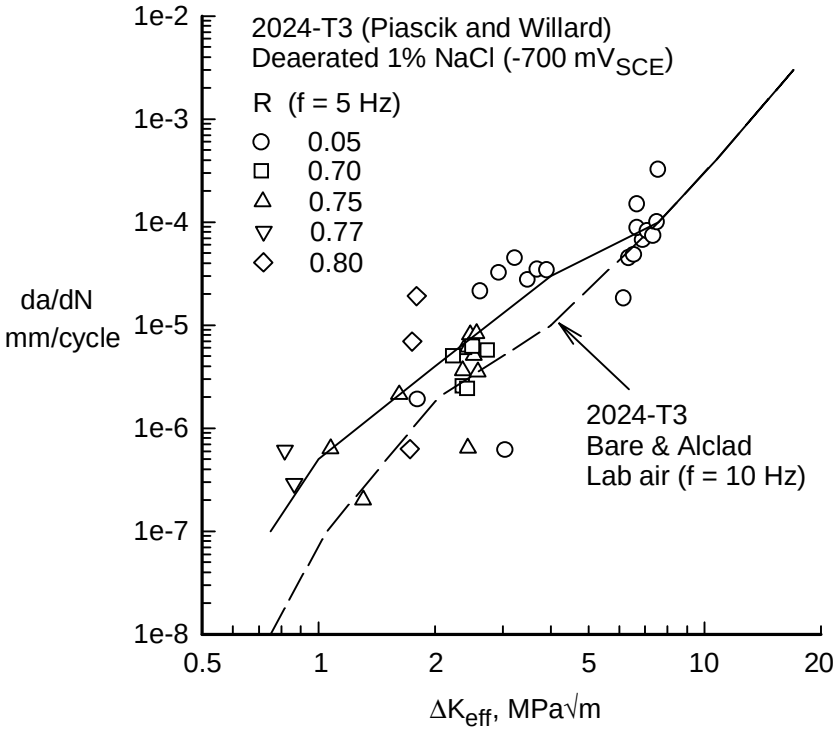

Figure 7. – Comparison of small- and large-crack growth rates on 2024-T3 bare or clad alloy in deaerated NaCl solution or laboratory air.

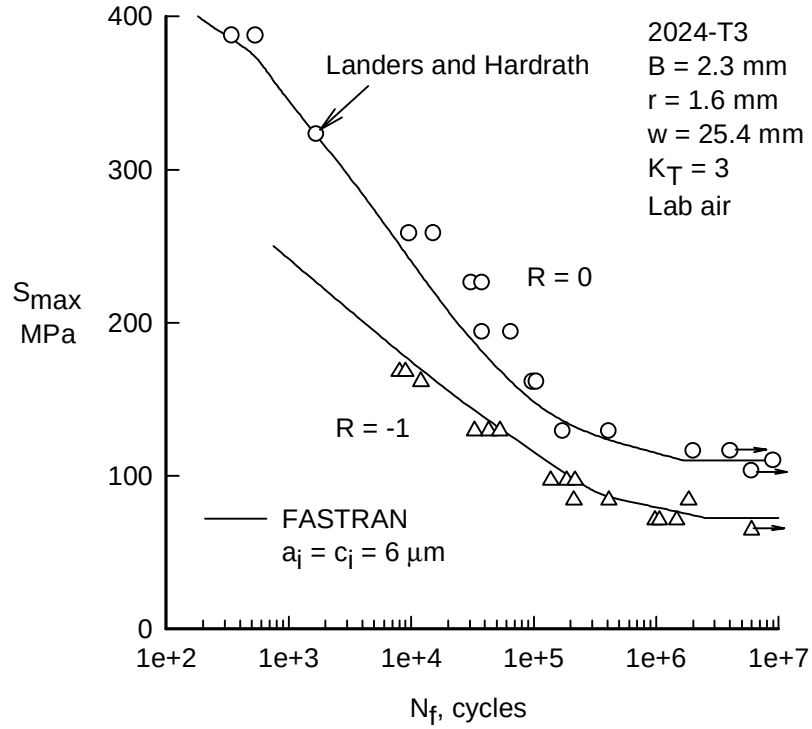

Figure 8. – Measured and calculated fatigue lives for 2024-T3 alloy circular-hole specimens.

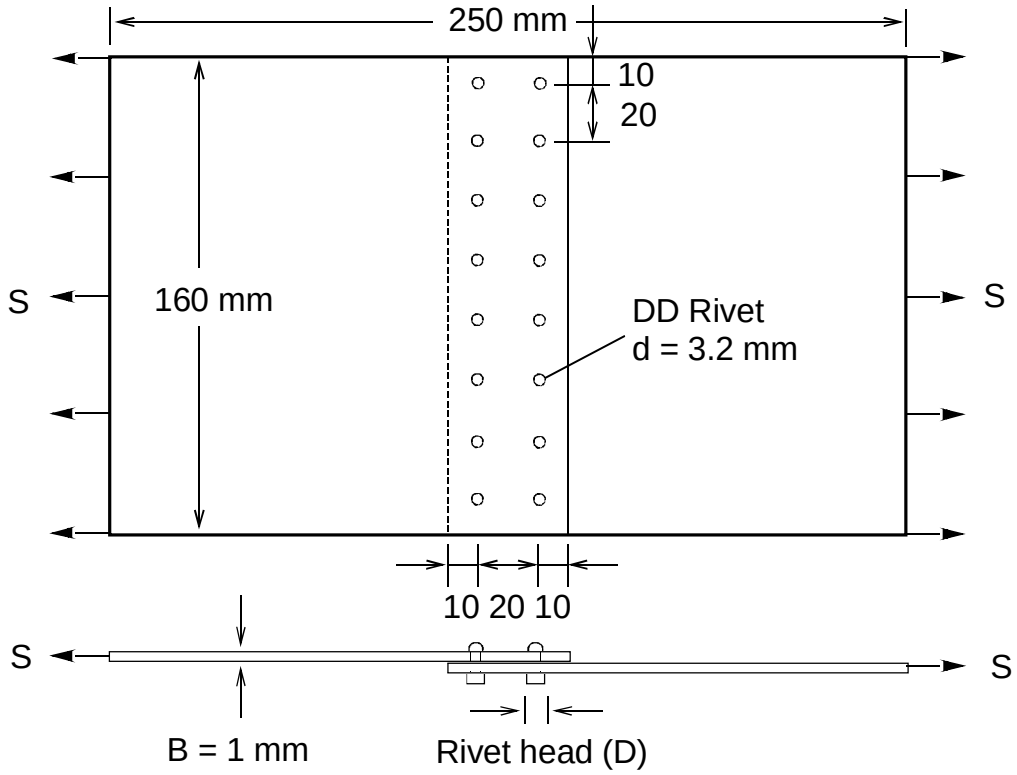

Figure 9. – Riveted lap joint specimen tested by Hartman [27].

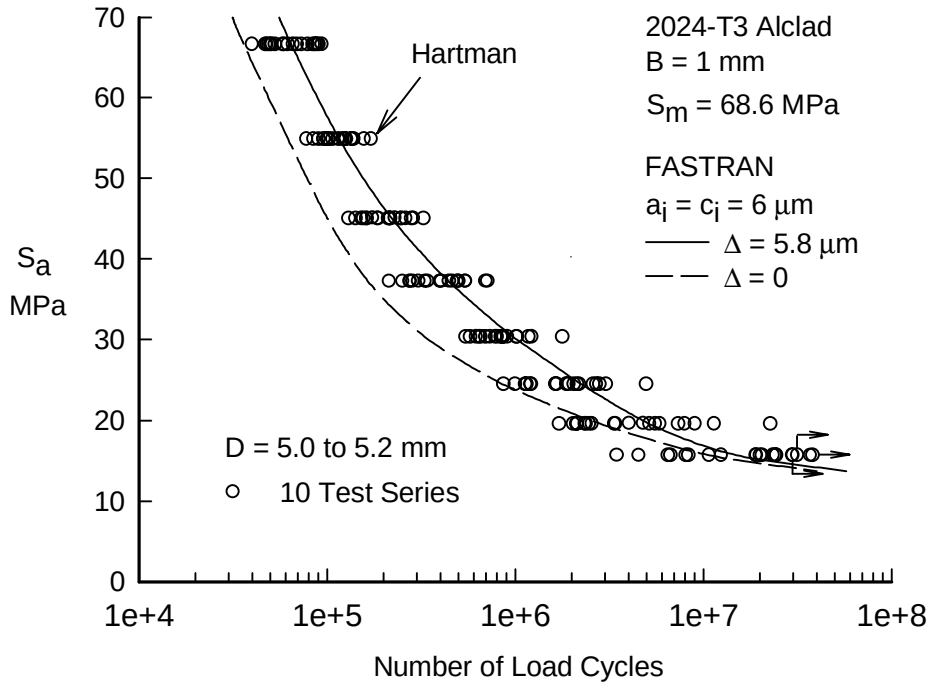

Figure 10. – Measured and calculated fatigue lives for NLR lap joint under constant-amplitude loading.

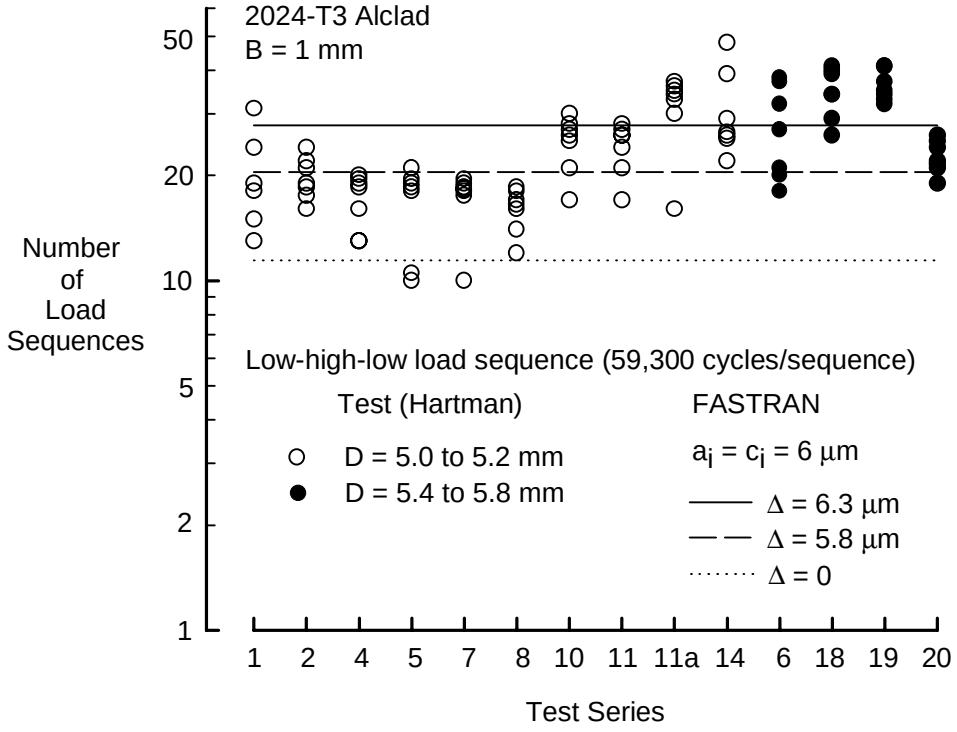

Figure 11. – Measured and predicted fatigue lives for NLR lap joint under low-high-low block loading sequence.

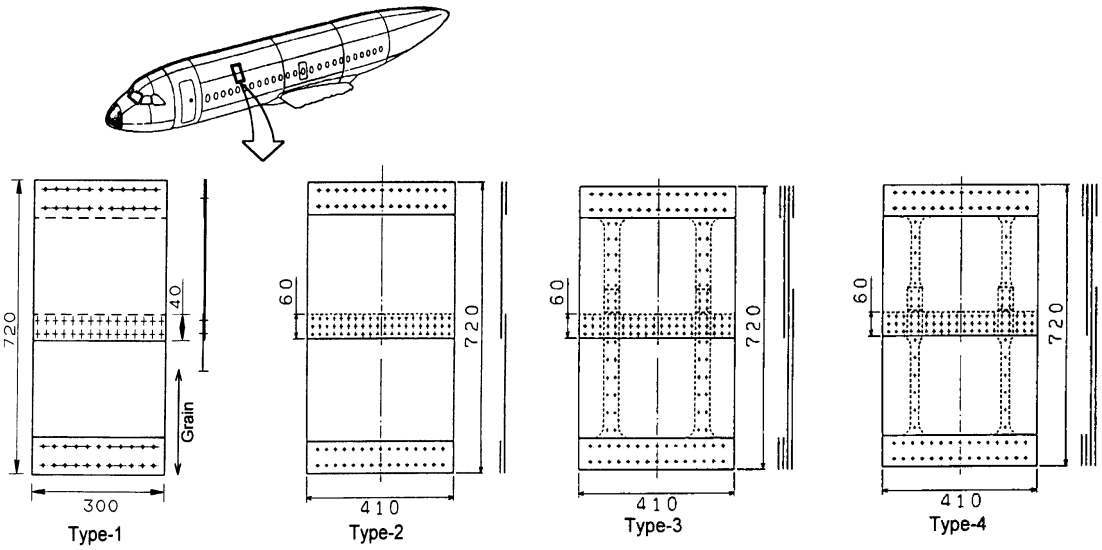

Figure 12. – Types of panel tests conducted by Furuta, Terada and Sashikuma [28].

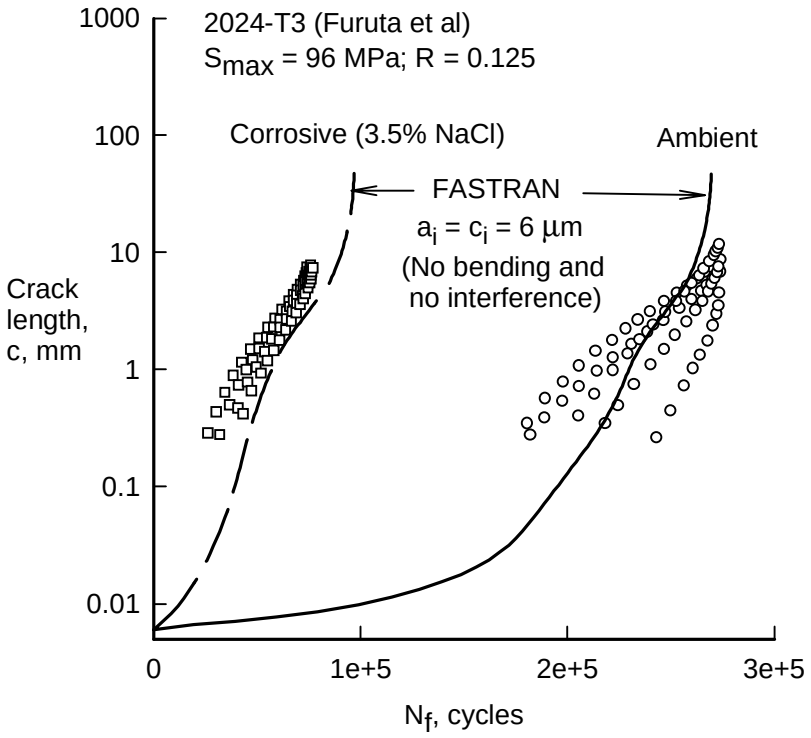

Figure 13. – Measured and calculated fatigue crack growth for Type 1 panels under ambient conditions and salt-water solution.

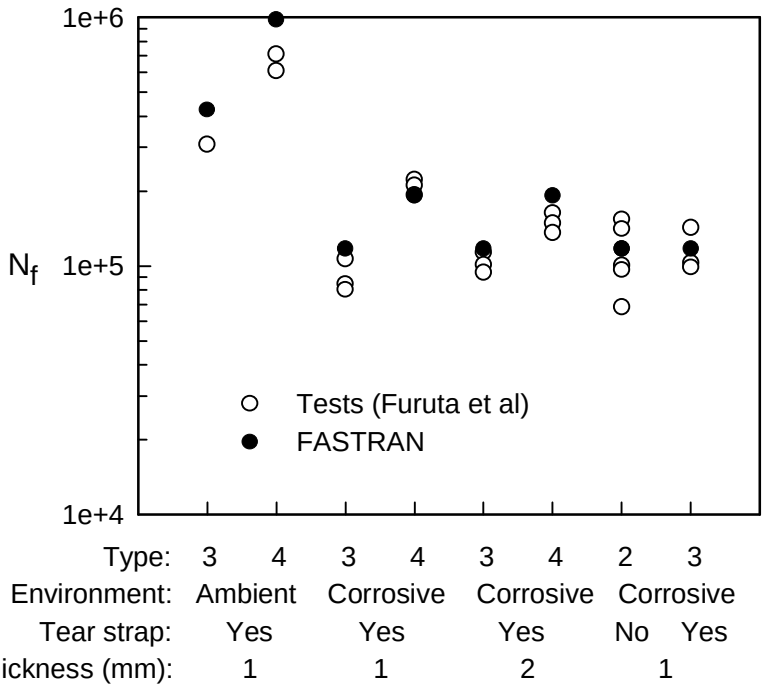

Figure 14. – Measured and calculated fatigue lives for various types of lap joints under ambient and corrosive (salt-water) media.

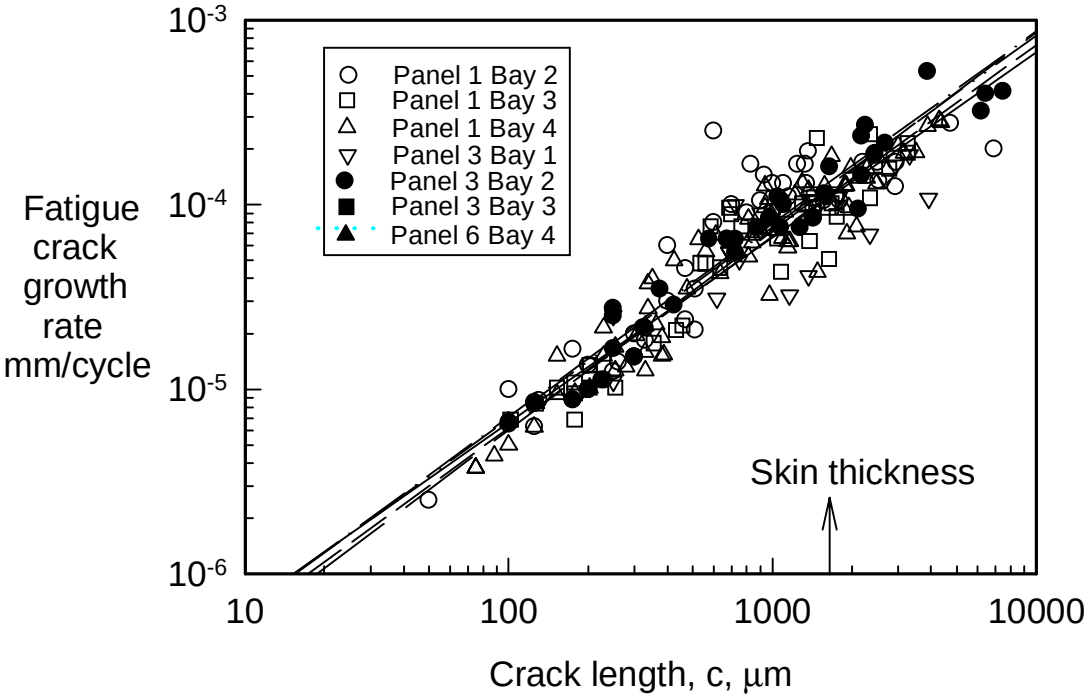

Figure 15. – Measured fatigue crack growth rates at rivets in aircraft fuselage lap joint.

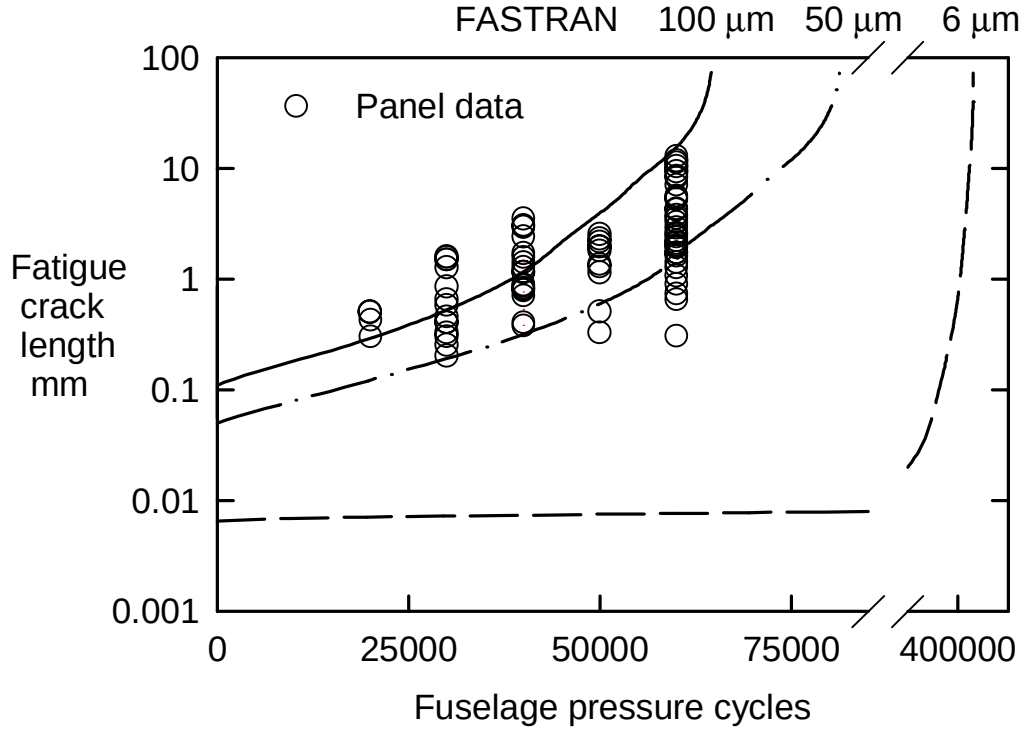

Figure 16. – Measured and calculated fatigue crack growth at rivets in aircraft fuselage lap joint.